

Design, production and reverse engineering of ultra-steep hot mirrors

Jinlong Zhang,^{1,2} Alexander V. Tikhonravov,³ Yongli Liu^{1,2}, Michael K. Trubetskov,^{3,4}
Artur Gorokh,³ and Zhanshan Wang^{1,2,*}

¹Key laboratory of advanced micro-structure materials, Ministry of Education, Shanghai, 200092, China

²Institute of Precision Optical Engineering, Department of physics, Tongji University, Shanghai, 200092, China

³Research Computing Center, Moscow State University, Leninskie Gory, 199992 Moscow, Russia

⁴Max Planck Institute of Quantum Optics, Hans-Kopfermann-Strasse 1, Garching 85748, Germany

*wangzs@tongji.edu.cn

Abstract: We present the whole design-production chain of an ultra-steep hot mirror produced using the indirect monochromatic monitoring technique. The hot mirror without thin layers is designed utilizing the stochastic optimization procedure that takes in account upper and lower constraints for layer optical thickness. We produced the hot mirror with the ion-assisted electron beam deposition technique using indirect monochromatic monitoring strategy, performed reverse engineering of the deposited coatings, and illustrated that the random variation of the tooling factors in low-index layers is the main factor causing production errors. We modified the monitoring strategy with low-index layers monitored by quartz crystal monitor, and demonstrated the excellent correspondence to the theoretical spectral performance.

©2014 Optical Society of America

OCIS codes: (310.1860) Deposition and fabrication; (310.4165) Multilayer design; (310.6860) Thin films, optical properties.

References and links

1. J. A. Dobrowolski, "Optical properties of films and coatings," in *Handbook of Optics*, M. Bass, ed. (McGraw-Hill, 2010), IV, pp. 7.15–7.53.
2. H. A. Macleod, *Thin-Film Optical Filters*, 4th ed. (CRC Press, 2010).
3. A. Thelen, "Design of a hot mirror: contest results," *Appl. Opt.* **35**(25), 4966–4977 (1996).
4. A. V. Tikhonravov, M. K. Trubetskov, and G. W. DeBell, "Application of the needle optimization technique to the design of optical coatings," *Appl. Opt.* **35**, 5493–5508 (2007).
5. A. V. Tikhonravov and M. K. Trubetskov, "Modern design tools and a new paradigm in optical coating design," *Appl. Opt.* **51**(30), 7319–7332 (2012).
6. A. V. Tikhonravov, M. K. Trubetskov, I. Kozlov, S. Alekseev, P. Konotopov and V. Zhupanov, "Correlated choice of design and monitoring strategy," in *Optical Interference Coatings*, OSA Technical Digest Series (Optical Society of America, 2013), paper WB3.
7. S. Wilbrandt, O. Stenzel, and N. Kaiser, "All-oxide broadband antireflection coatings by plasma ion assisted deposition: design, simulation, manufacturing and re-optimization," *Opt. Express* **18**(19), 19732–19742 (2010).
8. T. V. Amotchkina, M. K. Trubetskov, V. Pervak, and A. V. Tikhonravov, "Design, production, and reverse engineering of two-octave antireflection coatings," *Appl. Opt.* **50**(35), 6468–6475 (2011).
9. T. V. Amotchkina, S. Schlichting, H. Ehlers, M. K. Trubetskov, A. V. Tikhonravov, and D. Ristau, "Computational manufacturing as a key element in the design-production chain for modern multilayer coatings," *Appl. Opt.* **51**, 7604–7615 (2011).
10. C. J. van der Laan, "Optical monitoring of nonquarterwave stacks," *Appl. Opt.* **25**(5), 753–760 (1986).
11. C. C. Lee, K. Wu, C. C. Kuo, and S. H. Chen, "Improvement of the optical coating process by cutting layers with sensitive monitoring wavelengths," *Opt. Express* **13**(13), 4854–4861 (2005).
12. B. Chun, C. K. Hwangbo, and J. S. Kim, "Optical monitoring of nonquarterwave layers of dielectric multilayer filters using optical admittance," *Opt. Express* **14**(6), 2473–2480 (2006).
13. T. V. Amotchkina, M. K. Trubetskov, V. Pervak, B. Romanov, and A. V. Tikhonravov, "On the reliability of reverse engineering results," *Appl. Opt.* **51**(22), 5543–5551 (2012).
14. A. V. Tikhonravov and M. K. Trubetskov, OptiLayer Thin Film Software, <http://www.optilayer.com>.
15. J. L. Zhang, Y. J. Xie, X. B. Cheng, H. F. Jiao, and Z. S. Wang, "Thin-film thickness-modulated designs for optical minus filter," *Appl. Opt.* **52**(23), 5788–5793 (2013).
16. J. L. Zhang, A. V. Tikhonravov, M. K. Trubetskov, Y. L. Liu, X. B. Cheng, and Z. S. Wang, "Design and fabrication of ultra-steep notch filters," *Opt. Express* **21**(18), 21523–21529 (2013).

17. T. V. Amotchkina, M. K. Trubetskov, V. Pervak, S. Schlichting, H. Ehlers, D. Ristau, and A. V. Tikhonravov, "Comparison of algorithms used for optical characterization of multilayer optical coatings," *Appl. Opt.* **50**(20), 3389–3395 (2011).
 18. A. V. Tikhonravov, M. K. Trubetskov, T. V. Amotchkina, G. DeBell, V. Pervak, A. K. Sytchkova, M. L. Grilli, and D. Ristau, "Optical parameters of oxide films typically used in optical coating production," *Appl. Opt.* **50**(9), C75–C85 (2011).
-

1. Introduction

Hot mirrors are optical filters with a cutoff at 700 nm which transmit the visible radiation from 400 to 700 nm without disturbing the color balance, and reflect the near infrared spectral light [1, 2]. Such filters have various scientific and technological applications, including optical systems in projection and illumination systems, and specialized applications in fluorescence microscopy.

Researchers have reported many studies of the design and production of hot mirrors. At the topical meeting on optical interference coatings in 1995, the design problem was a hot mirror to improve the efficacy of tungsten lamps [3]. Several designs of hot mirrors with excellent spectral properties were presented in [4], but all these designs had several thin layers with optical thicknesses of about 20–30 nm. To avoid thin design layers, a special stochastic optimization technique has been proposed [5]. This technique allows one to obtain hot mirror designs without thin layers. An example of deposition of a hot mirror without thin layers using indirect broadband monitoring strategy was presented in [6].

The main goal of our present study is to design and produce optimal hot mirror with a stable deposition process controlled by indirect monochromatic monitoring technique. In recent years several researchers have presented results on the modern design-production chains of multilayer coatings [7–9], including design selection, choosing monitoring technique, computational manufacturing, coating production, reverse engineering of the deposited coatings that provides a feedback to the deposition process. However, the previous studies are mostly based on the broadband monitoring, and the design-production chain for the widely used indirect monochromatic monitoring system has not been reported yet.

In order to obtain a practical hot mirror design without thin layers the stochastic constrained optimization was applied [5]. The reasons for designing optical coatings without thin layers are widely known. Conventional deposition processes impose practical limitations on physical layer thicknesses [7]. Lower constraints on thicknesses can be also applied in connection with monitoring strategies used for coating production. Such constraints are especially desirable to minimize thickness errors in the level monitoring technique [10–12]. The upper constraints for individual layer thicknesses may help to avoid essential changes of film structure and unreasonably high total optical thickness values.

We produced experimental samples using the ion-assisted electron-beam deposition technology. It possesses the advantages of high deposition rate, good stress quality, and high stability of the refractive indices. The indirect monochromatic monitoring technique was used to control layer thicknesses.

We performed the reverse engineering of the produced hot mirror on the basis of off-line transmittance data [13] and found the most essential factors causing production errors. Based on this information, we modified monitoring strategy. As the result an essential decrease in discrepancy between the theoretical and measured data was achieved.

2. Theoretical design and determination of tooling factors

We considered a hot mirror with the performance that should satisfy the following demands under normal incidence: target transmittance of 100% (no back side reflections included) in the wavelength ranges of 400–690 nm, and target transmittance of 0% in the spectral region from 720 to 1150 nm, the wavelength step for target specification was 2 nm, as shown by the red dots in Fig. 1. In the design process we used Ta₂O₅ and SiO₂ as the high-index and low-index materials respectively, and the refractive indices of these materials are presented in Fig. 2. The substrate was B270 of 1.5 mm thickness, and the incident medium was air.

For designing of the hot mirror we applied the stochastic constrained optimization [5]. The lower and upper constraints for layer optical thicknesses were 100 and 350 nm. Since the refractive index of Ta_2O_5 is lower than the refractive index of TiO_2 used in [5], the number of layers for the stochastic optimization procedure was 44. The final design was obtained using OptiLayer software [14]. The layer thicknesses and spectral response of the final design are shown in Fig. 1. The average transmittance is higher than 98% in the pass spectral region, and the reflectance is higher than 99% in the wavelength region of 720–1150 nm.

The main structure of the final design can be interpreted as two short-wave pass eighth-wave/quarter-wave/eighth-wave stacks with the central rejection wavelength of about 800 nm and 1000 nm. The H L/2 layer pair is inserted between the substrate and the stack as a broadband anti-reflection (AR) coating to reduce oscillations in the pass band [15]. The obtained design has no thin layers, and as explained before the absence of thin design layers is suitable for accurate monitoring during the deposition.

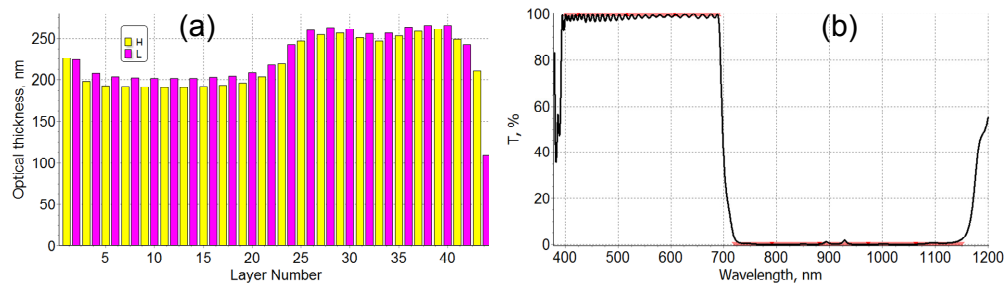


Fig. 1. Layer-thickness profile (a) and spectral transmittance (b) of an ultra-steep hot mirror obtained by stochastic constrained optimization.

For the coating production we used the Oporun Electron-beam deposition plant. During deposition layers were densified with an RF-type ion source. Thereby, the selected deposition parameters resulted in coatings without any relevant shift after cooling and venting. The indirect monochromatic back-reflection optical monitor was utilized to control thicknesses of deposited layers. Along with optical monitoring quartz crystal monitoring was performed in parallel, quartz crystal monitoring was mainly used as feedback for stabilizing evaporation rates and also for registering layer thicknesses (see also [16]).

In the case of indirect optical monitoring technique, a preliminary calibration should be done by pre-production depositions of single Ta_2O_5 and SiO_2 layers aimed at accurate determination of tooling factors and refractive indices wavelength dependencies. We deposited SiO_2 film and Ta_2O_5 film monitored at the wavelength of 650 nm that is approximately average value among monitoring wavelengths (see Section 3). Depositions of both film pairs were terminated at a swing level of 50% after the monitoring signals passed two minima and two maxima before termination instants.

After the deposition, spectral responses of the produced samples were measured using Cary5000 spectrophotometer, and the refractive indices and thicknesses were derived using OptiChar characterization software [14]. Thicknesses of the films on the monitor glasses were derived from the swing level, and the ratios of the above thicknesses were used to define tooling factors. The application of homogeneous film models for processing of measurement data was validated in our previous paper [16].

Figure 2 presents obtained wavelength dependencies of the refractive indices of the Ta_2O_5 and SiO_2 films. They are shifted upwards from the previously used in [16] dependencies for approximately 0.01 (0.5% relative difference) and 0.005 (0.3% relative difference) respectively. These differences are rather small and can be connected with systematic errors in reflectance data. Therefore the refractive indices in our deposition technique are quite reproducible from run to run.

The swing level of 50% corresponds to the 3.538 and 3.565 QWOT thicknesses of Ta_2O_5 and SiO_2 films on the monitoring glass. From the analysis of spectral data the thicknesses of

the Ta₂O₅ and SiO₂ films on the calotte were found to be 3.635 and 3.893 QWOT, respectively. This gives tooling factors equal to 0.973 and 0.916 for Ta₂O₅ and SiO₂ layers, respectively. These values are in remarkable correspondence with tooling factors in [16].

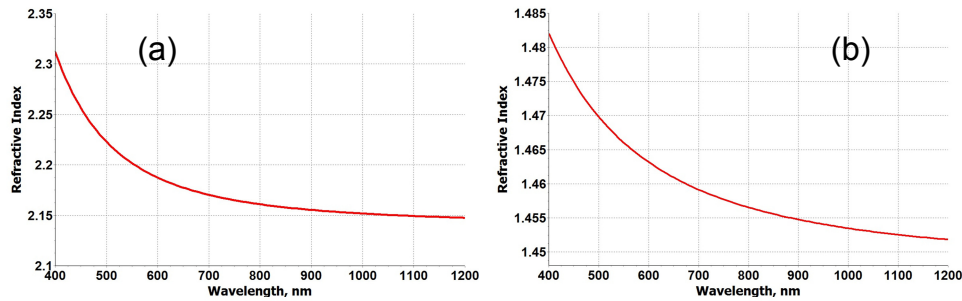


Fig. 2. Wavelength dependence of the refractive index of the Ta₂O₅ (a) and SiO₂ (b) films found in the frame of the homogeneous thin film model.

Additionally, we derived the tooling factors of quartz crystal monitor from single layers experiment. The actual layer physical thickness can be calculated in the optical characterization procedure, the thicknesses of the films on the quartz crystal monitor were registered during the deposition, and the ratios of the above thicknesses were used to define tooling factors of quartz crystal monitor. They are 0.945 and 0.856 for Ta₂O₅ and SiO₂ films respectively.

3. Monitoring strategy and results of the first coating run

In the first experiment we used the indirect monochromatic back-reflection monitoring with level monitoring method to control layer thicknesses. The monitoring strategy was using one monitoring chip to control thicknesses of two subsequent high and low index layers, and 22 chips were used in the whole deposition procedure. The main goal of using several monitoring chips instead of one monitoring chip is to prevent the accumulation of errors in the determination of an instant when a layer deposition should be terminated [10].

We used the new monitoring strategy option of OptiLayer software to select a proper sequence of monitoring wavelengths for all monitoring chips with an attempt to improve an accuracy of registration of termination instants. The criterion for choosing the monitoring wavelength is that the monitoring signal of each layer should pass at least one extremum and that the difference between the termination level and last registered signal extremum should be in the range of 20%–80% of the difference between previous signal extrema. In this case the reflectance is most sensitive to variations in the thickness of a deposited layer.

Table 1. Assignments of monitoring wavelengths for witness chips

Chips number	1	2-10	11	12	13-21	22
Wavelength/nm	645	570	605	645	730	475

We specified that 5 different wavelengths can be used in the monitoring. It was found that results for the most layer pairs met the criterion except the last one. Then we modified the monitoring wavelength for the last chip manually. In the final monitoring spreadsheet, one maximum was registered for all high-index layers and one minimum was registered for all low-index layers. The monitoring wavelengths for the witness chips of the hot mirror are shown in Table 1, and one can see that the wavelengths of 570nm and 730nm are most often presented, and only 4 layer pairs use different wavelengths.

We produced the hot mirror with the monitoring spreadsheet described above. After the deposition, transmittance of the sample was measured at normal incidence in the spectral range from 350 nm to 1200 nm using Cary5000 spectrophotometer. The measured transmittance of the manufactured hot mirror is depicted in Fig. 3, where the theoretical transmittance calculated by taking into account the backside reflectance from the B270 substrate is also presented. In this figure a good agreement between theoretical and

experimental data is observed. However, there is still observable discrepancy between experimental and theoretical transmittance curve, especially in the range 1150–1200 nm. This indicates the presence of considerable errors in layer parameters.

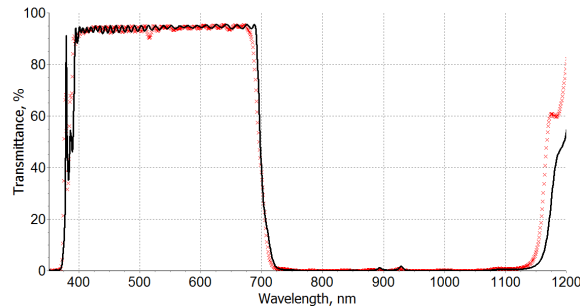


Fig. 3. Comparison of measured transmittance data (red crosses) and theoretical transmittance (solid black curve) of the hot mirror.

4. Reverse engineering and re-deposition with modified monitoring strategy

Although we produced the hot mirror with good performance, there were still some observed inconsistencies between experimental and theoretical transmittance data. The main purpose to perform reverse engineering was to find possible reasons of the observed deviations, and to correct the monitoring strategy in order to improve the monitoring accuracy.

In this experiment we used stable deposition process that produces high density films. Refractive indices of Ta_2O_5 and SiO_2 thin-film materials have been found with a high accuracy and verified using reliable results of the previous studies [17, 18]. This allows us to neglect possible small offsets in layer refractive indices and to attribute the observed deviations to errors in layer thicknesses.

According to our monitoring strategy, one chip was used to control two subsequent high-index and low-index layers, and layer depositions were terminated according to theoretically predicted swing levels. It can be theoretically shown that such monitoring strategy provides an accurate control of first high-index layers even in the presence of signal drifts. However, it is not possible to make the same statement with respect to low-index layers that are second layers of monitored layer pairs. The low-index layers followed the high-index layers, so the deposition of low-index layer can be significantly affected by the thickness errors of high-index layers and the shift of the measured signal. Thus it is reasonable to assume that the deviations observed in Fig. 3 can be attributed to thickness errors in low-index layers.

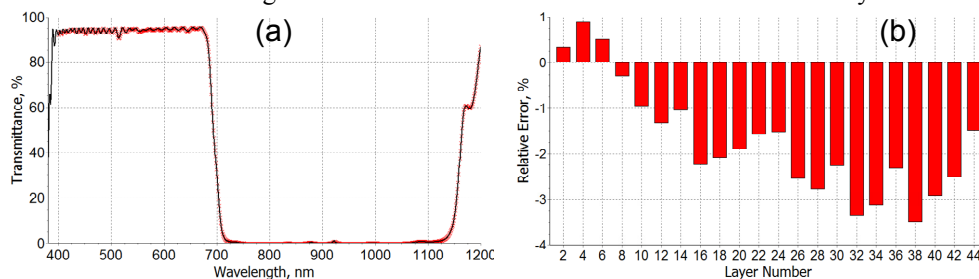


Fig. 4. (a) Fitting of measured hot mirror transmittance (red crosses) by the model transmittance (solid curve) when the model with random errors in thicknesses of low-index layers was applied. (b) The relative random errors in low-index layers determined by the reverse engineering procedure.

We performed reverse engineering of the produced hot mirror sample with OptiRE software [14] using the above assumption. Figure 4(a) shows the fitting of measured hot mirror transmittance by the model transmittance when the model with random errors in thicknesses of low index layers was applied. Relative errors in all low-index layers are shown

in Fig. 4(b). It is seen that the errors in all layers varied gradually during the deposition procedure, and the maximum errors were in the range of 3.5% of planned theoretical layer thicknesses. The achieved excellent fitting of measurement data confirms that deviations observed in Fig. 4(a) could be indeed attributed to errors in low index layers. The results indicate that errors in the thicknesses of low index layers were increasing in the course of coating deposition. Our analysis suggests that these errors were connected with a calibration drift caused by some inaccuracies of the mechanical setup of our monitoring scheme.

In order to verify the reliability of our analysis, we produced new sample of the hot mirror. Based on the analysis and the reverse engineering results, the thickness monitoring of high-index layers is stable and accurate. Thus it is reasonable to change monitoring technique for the low-index layers to further improve the spectral performance. We proposed to use quartz crystal monitor to control these thicknesses. In our deposition plant, there are six crystals and the deposition rate is quite stable which allows one to believe that the quartz crystal monitor can be used to monitor the low-index layers with an accuracy better than that in the previous optical monitoring strategy. So we produced the hot mirror without changing the monitoring parameters of high-index layers and the thicknesses of low-index layers were controlled by the quartz crystal monitor with the tooling factor of 0.856. In Fig. 5 we compare the measured transmittance data of the sample produced using this monitoring approach and theoretical transmittance data. In this figure an excellent agreement between theoretical and experimental data is observed, even for the small ripples in the transmission band. The obtained results confirm that random errors in low-index layers were the main inaccuracy factors in the previous deposition run.

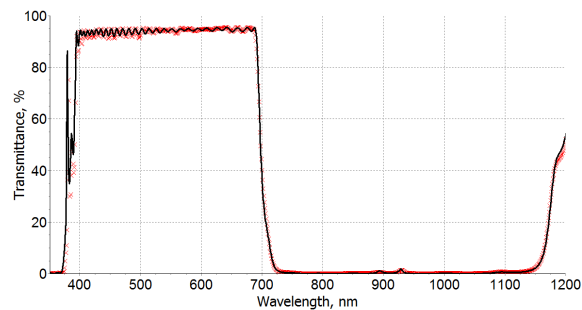


Fig. 5. Comparison of measurement transmittance data (red crosses) and theoretical transmittance (solid black curve) of the hot mirror in the second coating run.

5. Conclusion

In summary, we provided the whole design-production chain and successfully produced the high quality hot mirror. We designed the hot mirror without thin layers using stochastic optimization and produced it using indirect monochromatic monitoring strategy with conventional deposition technology. The reverse engineering was performed to demonstrate that the monitoring procedure provided an accurate control of the high-index layers, and that the remaining deviations from the target curve were due to errors in the low-index layers. Based on the feedback provided by the reverse engineering procedure we performed experiment with a modified monitoring strategy, and obtained an excellent correspondence with the theoretical spectral performance.

Acknowledgments

This work was partly supported by the National Natural Science Foundation of China (Grant Nos. 61235011, 61108014, 61205124), and the National 863 Program.